



9-2010

rAAV2/5 Gene-Targeting to Rods: Dose-Dependent Efficiency and Complications Associated With Different Promoters

William Beltran

University of Pennsylvania, wbeltran@vet.upenn.edu

Sanford L. Boye


Shannon E. Boye

Vince A. Chiodo

Alfred S. Lewin

See next page for additional authors

Follow this and additional works at: https://repository.upenn.edu/vet_papers

 Part of the [Eye Diseases Commons](#), [Medical Genetics Commons](#), [Ophthalmology Commons](#), and the [Veterinary Medicine Commons](#)

Recommended Citation

Beltran, W., Boye, S. L., Boye, S. E., Chiodo, V. A., Lewin, A. S., Hauswirth, W. W., & Aguirre, G. D. (2010). rAAV2/5 Gene-Targeting to Rods: Dose-Dependent Efficiency and Complications Associated With Different Promoters. *Gene Therapy*, 17 (9), 1162-1174. <http://dx.doi.org/10.1038/gt.2010.56>

This paper is posted at ScholarlyCommons. https://repository.upenn.edu/vet_papers/94
For more information, please contact repository@pobox.upenn.edu.

rAAV2/5 Gene-Targeting to Rods: Dose-Dependent Efficiency and Complications Associated With Different Promoters

Abstract

A prerequisite for using corrective gene therapy to treat humans with inherited retinal degenerative diseases that primarily affect rods is to develop viral vectors that target specifically this population of photoreceptors. The delivery of a viral vector with photoreceptor tropism coupled with a rod-specific promoter is likely to be the safest and most efficient approach to target expression of the therapeutic gene to rods. Three promoters that included a fragment of the proximal mouse opsin promoter (mOP), the human G-protein-coupled receptor protein kinase 1 promoter (hGRK1), or the cytomegalovirus immediate early enhancer combined with the chicken β actin proximal promoter CBA were evaluated for their specificity and robustness in driving GFP reporter gene expression in rods, when packaged in a recombinant adeno-associated viral vector of serotype 2/5 (AAV2/5), and delivered via subretinal injection to the normal canine retina. Photoreceptor-specific promoters (mOP, hGRK1) targeted robust GFP expression to rods, whereas the ubiquitously expressed CBA promoter led to transgene expression in the retinal pigment epithelium, rods, cones and rare Müller, horizontal and ganglion cells. Late onset inflammation was frequently observed both clinically and histologically with all three constructs when the highest viral titers were injected. Cone loss in the injected regions of the retinas that received the highest titers occurred with both the hGRK1 and CBA promoters. Efficient and specific rod transduction, together with preservation of retinal structure was achieved with both mOP and hGRK1 promoters when viral titers in the order of 10^{11} vg ml⁻¹ were used.

Keywords

rAAV vectors, promoters, rod, retina, gene transfer, dog

Disciplines

Eye Diseases | Medical Genetics | Ophthalmology | Veterinary Medicine

Author(s)

William Beltran, Sanford L. Boye, Shannon E. Boye, Vince A. Chiodo, Alfred S. Lewin, William W. Hauswirth, and Gustavo D. Aguirre

Published in final edited form as:

Gene Ther. 2010 September ; 17(9): 1162–1174. doi:10.1038/gt.2010.56.

rAAV2/5 gene-targeting to rods: dose-dependent efficiency and complications associated with different promoters

William A. Beltran, DVM, PhD¹, Sanford L. Boye, MS², Shannon E. Boye, PhD², Vince A. Chiodo, BS², Alfred S. Lewin, PhD³, William W. Hauswirth, PhD², and Gustavo D. Aguirre, VMD, PhD¹

¹ Section of Ophthalmology, Department of Clinical Studies School of Veterinary Medicine, University of Pennsylvania, Philadelphia, PA

² Department of Ophthalmology, University of Florida, Gainesville, FL

³ Department of Molecular Genetics and Microbiology, University of Florida, Gainesville, FL

Abstract

A prerequisite for using corrective gene therapy to treat humans with inherited retinal degenerative diseases that affect primarily rods is to develop viral vectors that target specifically this population of photoreceptors. The delivery of a viral vector with photoreceptor tropism coupled with a rod-specific promoter is likely to be the safest and most efficient approach to target expression of the therapeutic gene to rods. Three promoters that included a fragment of the proximal mouse opsin promoter (mOP), the human G-protein coupled receptor protein kinase 1 promoter (hGRK1), or the cytomegalovirus immediate early enhancer combined with the chicken beta actin proximal promoter CBA) were evaluated for their specificity and robustness in driving GFP reporter gene expression in rods, when packaged in a recombinant adeno-associated viral vector of serotype 2/5 (AAV2/5), and delivered via subretinal injection to the normal canine retina. Photoreceptor specific promoters (mOP, hGRK1) targeted robust GFP expression to rods, while the ubiquitously expressed CBA promoter led to transgene expression in the retinal pigment epithelium, rods, cones and rare Müller, horizontal and ganglion cells. Late onset inflammation was frequently observed both clinically and histologically with all three constructs when the highest viral titers were injected. Cone loss in the injected regions of the retinas that received the highest titers occurred with both the hGRK1 and CBA promoters. Efficient and specific rod transduction, together with preservation of retinal structure was achieved with both mOP and hGRK1 promoters when viral titers in the order of 10^{11} vg/ml were used.

Keywords

rAAV vectors; promoters; rod; retina; gene transfer; dog

Users may view, print, copy, download and text and data- mine the content in such documents, for the purposes of academic research, subject always to the full Conditions of use: http://www.nature.com/authors/editorial_policies/license.html#terms

Correspondence: Dr. William A. Beltran, Section of Ophthalmology, Department of Clinical Studies School of Veterinary Medicine, University of Pennsylvania, 3900 Delancey street, Philadelphia, PA, 19104, USA., Phone: 1 215 898 4692, Fax: 1 215 573 2162, wbeltran@vet.upenn.edu.

CONFLICT of INTEREST: WWH and the University of Florida have a financial interest in the use of rAAV therapies, and own equity in a company (AGTC Inc.) that might, in the future, commercialize some aspects of this work. All remaining authors declare that they have no competing financial interests.

INTRODUCTION

With substantial evidence from studies conducted in animal models^{1–3} that the retinal pigment epithelium (RPE) can be efficiently transduced for corrective gene therapy in humans^{4–6}, emphasis has now shifted at developing and evaluating viral vectors that will enable targeting other retinal cell populations. The need for efficient and safe viral vector constructs with specific photoreceptor (PR) tropism is essential for targeting retinal degenerative diseases such as retinitis pigmentosa, cone dystrophies, cone-rod dystrophies, and the non-exudative form of age-related macular degeneration.

Adeno-associated viruses (AAV) are the most commonly used vectors in retinal gene therapy as they offer several advantages over other viral vectors, e.g. low immunogenicity, prolonged transgene expression, and ability to transduce postmitotic cells. There are currently nine different AAV serotypes (1–9) commonly used as vectors.⁷ The discovery that their specific cell tropism is under the control of their capsid proteins has led to the development of chimeric recombinant AAV (rAAV) serotypes (also termed pseudotypes).⁸ These vectors are generated by inserting the promoter, transgene, and poly-A site of interest between two AAV2 internal terminal repeats (ITRs), and packaging the DNA vector into the desired capsid serotype.

Large animal models such as the dog have been used by several groups both to confirm cell tropism, and to demonstrate proof of principle of viral-mediated gene therapies. To this date, 5 different rAAV chimeric serotypes (rAAV2/1, rAAV2/2, rAAV2/4, rAAV2/5, and rAAV2/8) have been tested in the canine retina (for review see ⁹), and of these, only rAAV2/2, rAAV2/5 and rAAV2/8 target, albeit not specifically, PR cells. rAAV2/2 has been used by several groups to transduce the RPE in a canine model of Leber's congenital amaurosis,^{1, 10, 11} yet a single study has reported that in this species rAAV2/2 may also target PRs, and a small number of ganglion cells.¹² In a study that examined the tropism of a rAAV2/8 delivered to the canine retina via subretinal injection, the authors reported GFP expression in the RPE, PRs, inner nuclear layer (INL) and ganglion cells. GFP was also found in the brain along the visual pathway, and detection of the vector genome by PCR in the lateral geniculate nucleus, optic radiations, and visual cortex suggested that this vector has the potential for transfer across synapses.¹³ For obvious safety reasons, the widespread dissemination of this virus may limit its use for PR gene therapy in human patients.

Although rAAV2/5 has a slower onset of transgene expression than that of rAAV2/8,¹⁴ it is a promising vector for PR targeting. Indeed, several groups have demonstrated high efficiency transduction of both RPE and PRs with this serotype,^{15–17} and it has been shown to target GFP expression to cones when specific cone promoters are incorporated in the construct.^{18–21}

The use of a constitutively expressed promoter in rAAV2/2, rAAV2/5, and rAAV2/8 vectors has been shown to drive expression of the reporter gene in PRs but also in the RPE and inner retinal cells.^{12, 22} To further restrict transgene expression to a particular retinal cell type, substantial effort is now being placed on identifying and validating promoters that are activated specifically in the cell of interest. The choice of a particular rAAV serotype coupled with a cell-specific promoter is currently considered as the safest approach to achieve sustained transgene levels while avoiding off-target expression.

The availability of a panel of viral constructs with different promoters that can drive the expression of a transgene in both rods and cones, or alternatively, in subpopulations of these PRs, is a prerequisite for developing efficient and safe gene therapies. Viral vectors that target cones have been developed,²¹ and are currently being used in a canine model of achromatopsia,²³ yet there is currently a dearth of vectors that target rods. This study

examined the efficiency of three rAAV2/5 constructs, and reports rod-specific expression in the normal adult canine retina with a mouse opsin (mOP) promoter, or a human G-protein-coupled receptor protein kinase 1 (hGRK1) promoter, while transgene expression was found in rods, cones, and other non-photoreceptor retinal cells when a constitutive chicken beta actin (CBA) promoter was used.

RESULTS

Clinical evaluation and histopathology

Subretinal injections performed through a transvitreal approach without vitrectomy enabled injection of 150 μ l of viral vector preparation in young adult canine eyes. This resulted in subretinal blebs in 10/14 eyes that covered up to 1/4 of the entire retinal surface (Figure 2A). In two eyes (E1048-L; E1055-L) a subretinal bleb was formed but some viral vector solution entered under the RPE (sub-RPE). This could be clearly observed during the injection by noticing the sudden and localized persistent pink/copper discoloration of the tapetal fundus. In one eye (E1053-L), despite a successful retinotomy, the entire injected volume failed to form a subretinal bleb, and refluxed into the vitreous. Finally, in another eye (P1476-R) a small amount of viral solution went sub-RPE, and the rest refluxed into the vitreous. These eyes were included in the study to examine the effects of sub-optimal or failed subretinal injections. As noted in Table 1, these eyes showed intense GFP expression in rods, although in most cases, the area of coverage was reduced to the immediate injection site.

Clinical assessment throughout the injection-termination period revealed a number of fundus abnormalities with all three constructs. Focal signs of inflammation (retinitis, chorioretinitis, or vasculitis) in the injected area occurred only with the highest viral titers ($\sim 10^{12} - 10^{13}$ vg/ml), and were seen in (6/10 eyes). Another common finding that was observed in eyes treated with either high or low viral titers was an increase in the diameter of retinal vessels (6/16 eyes) that was not limited to the injection site. In two retinas (E1055-R, and E1050-R) that had reattached well shortly after the formation of the subretinal bleb, a subsequent detachment was noted, at 48 and 26 days post-injection, respectively. As these detachments were temporally associated with the onset of inflammatory changes, they were not thought to have been surgically induced. With the exception of one eye (E1050-R), clinical signs were controlled with additional anti-inflammatory medications. The frequent late-onset of these retinal alterations (approx 6 weeks post-injection) suggests that these may have been triggered by an immune-mediated response.

Retinal histopathology

Retinal histopathology performed on H&E stained sections that included the region of the bleb as well as surrounding non-injected areas confirmed most of the clinical signs observed ophthalmoscopically (Figure 3).

rAAV2/5-mOP-GFP—With the mOP promoter histological anomalies were found with the two highest titers. The eye that received the highest titer (E1048-R; 3.27×10^{13} vg/ml) had a focal retinal atrophy in close proximity to the site of retinotomy. In surrounding regions, (Fig 3A₁₋₂) reduced density of PRs resulted in ONL thinning, and the remaining cells had shortened inner segments (IS; arrows) and disrupted outer segments (OS; asterisks). Lymphoplasmacytic cell infiltrates were seen throughout the inner retina length, and around blood vessels (Fig 3A₁₋₂, arrowheads), even at sites distant from the subretinal bleb. A 3.27×10^{12} vg/ml titer caused similar but less extended damage in eye E1048-L (Fig 3A₃). Focal regions of atrophy (asterisk), and perivascular cell infiltrates (arrowheads) were present but were surrounded by well-preserved retina. At the two lowest titers used (P1473-R; $3.27 \times$

10^{11} vg/ml; P1473-L: 3.27×10^{10} vg/ml), there was good structural preservation in the region of the bleb, and no invasion of the retina by inflammatory cells (Fig 3A₄).

rAAV2/5-hGRK1-GFP—In retinas treated with the highest titer (1.51×10^{13} vg/ml) of the construct that contained the hGRK1 promoter, variation in ONL thickness (E1055-R; Fig 3B₁), loss of IS/OS (E1055-R; Fig 3B₂, asterisks), and retinal atrophy (E1055-R; not shown) were observed in localized regions within the bleb area. Lymphoplasmacytic perivascular cell infiltrates (Fig 3B₂, arrowheads) were seen predominantly in the injected areas of all eyes that received the highest titer, as well as in P1476-L (1.51×10^{12} vg/ml; Fig 3B₃, arrowheads), consistent with the observed clinical findings (Table 1). Sections stained with H&E showed good preservation of the retinal structure both in the injected and non-injected areas of eyes treated with titers of 1.51×10^{12} vg/ml or lower (Fig 3B₄).

rAAV2/5-CBA-GFP—Histopathological findings with the construct that included the CBA promoter showed some of the most severe retinal alterations when the two highest titers (4.79×10^{13} and 4.79×10^{12} vg/ml) were used. This included localized retinal atrophy and detachment in E1050-R (4.79×10^{13} vg/ml; Fig 3C₁), perivascular and inner retinal infiltration with lymphocytes and plasmocytes (Fig 3C₂, arrowheads), loss of PR OS (Fig 3C₃, asterisks) and shortened IS (Fig 3C₃, arrows) in eye E1050-L (4.79×10^{12} vg/ml). Absence of perivascular infiltrates and preserved retinal structure was seen in eye P1475-R treated with a lower titer of 4.79×10^{11} vg/ml (Fig 3C₄), and in eye P1475-L that received the lowest titer (4.79×10^{10} vg/ml).

In summary, clinical and histopathological signs of inflammation were seen with all three promoters. These were most severe when titers in the order of $10^{12} - 10^{13}$ vg/ml were used. Increased dilation of retinal vessels was the only clinical sign observed when constructs with the mOP and CBA promoters were used with the lowest titers ($\sim 10^{10} - 10^{11}$ vg/ml). This increase in vessel diameter appeared to have been transient or responsive to anti-inflammatory therapy, as no vascular abnormalities were detected by histology at termination.

Retinal transduction efficiency

rAAV2/5-mOP-GFP—GFP expression was observed with and without immunolabeling in all eyes, and was limited, predominantly, to rods in the retinal region where the subretinal bleb was formed (Fig 4). The intensity of GFP labeling was correlated to the dose of viral vector preparation. To compare the expression levels by vector dose, we selected for examination, areas at the center of the injected bleb. Preparations with the two highest titers (3.27×10^{13} , and 3.27×10^{12} vg/ml) resulted in intense labeling of the IS and ONL. With the exception of a single row of somatas located at the scleral side of the ONL, the remaining ONL nuclei were intensely labeled (Fig 4A₁₋₂, arrows). The potent GFP labeling in the central region of the previously formed bleb was associated with significant ONL thinning, particularly with the 3.27×10^{13} vg/ml titer. Faint signal was detected in the inner nuclear layer (INL) and ganglion cell layer (GCL) (data not shown), and by immunohistochemistry, GFP expression could also be detected in rod OS (Fig 4A₂, asterisks). Lower titers (3.27×10^{11} vg/ml) caused a decrease in staining intensity (Fig 4A₃), and only rare rods were found to express GFP at 3.27×10^{10} vg/ml (Fig 4A₄, arrows). With these two low titers no thinning of the GFP-labeled ONL was seen across the injected region. Confocal microscopy using a cone arrestin antibody which labels both S and L/M cones confirmed that the GFP expression in the ONL was restricted to rods since no colocalization was observed in somatas, IS or OS of cones (Fig 4B₁₋₃, arrows). In the transduced region of the E1048-R retina which had received the highest viral titer (3.27×10^{13} vg/ml), the morphology of cones was abnormal, and characterized by shortened and

enlarged IS, and disrupted OS (Fig 4B_{2,3}). This structural alteration was most likely secondary to rod loss and caused by decreased lateral support of cone OS/IS in the PR layer, and/or reduced production of rod-derived cone viability factors. Such changes were not seen in non-injected regions of this same retina (Fig 4B₄).

rAAV2/5-hGRK1-GFP—GFP expression was observed with and without immunolabeling in all injected eyes in the region where the subretinal bleb was formed, and was found to be primarily restricted to rods (Fig 5). When images were digitally captured with the same settings for exposure time and gain, the highest intensity of fluorescence was observed in the ONL, IS and OS of retinas treated with a titer of 1.51×10^{12} vg/ml (P1476-L; Fig 5A₂), while decreased labeling was seen with lower titers (Fig 5A₃₋₄). In eyes treated with the highest titer (1.51×10^{13} vg/ml) intensity of GFP labeling was lower than in those treated with a 10-fold lower dose, and was associated with reduced ONL thickness (Fig 5A₁), an indication of outer retinal damage associated with vector administration. Immunolabeling with an anti-GFP antibody showed a similar pattern as that observed with native GFP fluorescence, but in addition, also detected expression of the reporter gene in the OS (Fig 5A₂, asterisks). In one single eye (P1476-L; 1.51×10^{12} vg/ml), GFP expression was also detected in cells located on the vitreal side of the INL (Fig 5A₂, arrows), and GCL (Fig 5A₂, arrowhead), as well as in the IPL. Confocal microscopy revealed that in eyes treated with titers of 1.51×10^{12} vg/ml and lower, GFP expression could be seen throughout the ONL except in a single row of somatas located at the scleral side of the ONL (Fig 5B₁, arrows). Cone arrestin antibody labeling confirmed that this single row of somatas represented cones, and that GFP expression was restricted to rods (Fig 5B₂₋₃).

rAAV2/5-CBA-GFP—GFP expression was observed with and without any immunolabeling in all injected eyes in the region where the subretinal bleb was formed, and was found predominantly in RPE cells, rods, and cones (Fig 6A₁₋₄). The intensity of the labeling and number of cells expressing GFP was highest in the retina treated with a titer of 4.70×10^{11} vg/ml (Fig 6A₃). With higher titers, even though the fluorescence intensity of individual transduced cells was elevated, there was a moderate decrease in ONL thickness in the retina (E1050-L; 4.70×10^{12} vg/ml) (Fig 6A₂). In the eye (E1050-R) that received the highest titer (4.70×10^{13} vg/ml), an extended area of complete ONL loss was found, and GFP expression in PRs was observed only over a limited distance at the border of this area of atrophy (Fig 6A₁). This region of complete PR loss corresponded to the large area of retinal detachment that was observed histologically (Fig 3C₁). Immunolabeling with the GFP antibody confirmed transduction of the RPE, rods and cones but also showed that occasional horizontal (Fig 6A₃, arrows), ganglion, and Müller cells (Fig 6A₃, arrowheads) expressed the transgene. Staining of the inner plexiform layer (IPL) and nerve fiber layer (NFL) could also be detected, and extended far beyond the region of transduced PRs (data not shown).

Cone toxicity

In addition to the dose-dependent pathological alterations observed with the three viral constructs, cone-specific damage was found with vectors that carried the hGRK1 and CBA promoters.

rAAV2/5-hGRK1-GFP—In eyes that were subretinally injected with the highest titer of viral construct (E1053-R, E1055-R; 1.51×10^{13} vg/ml), there was a different pattern of GFP labeling than that observed with lower titers. In most of the injected area, GFP labeling was found throughout the entire thickness of the ONL (Fig 5C₁), and only in limited peripheral areas of the injected region, was a similar pattern of unlabeled cone somatas observed (E1053-R; data not shown). To determine whether the absence of an unlabeled layer of

somatas on the scleral side of the ONL resulted from GFP expression in cones or alternatively in the loss of this population of photoreceptors, double labeling with cone arrestin was performed. This showed a significantly reduced number of cells labeled with this marker, as well as a reduced intensity in the cone arrestin staining (Fig 5C₁₋₂). Careful examination of DAPI, and H&E stained sections revealed a drastically reduced density of large euchromatic cone nuclei (data not shown), thus confirming that cone loss occurred in the retinal area transduced by this viral construct when used at a titer of 1.51×10^{13} vg/ml. At the border of this region, between treated and non-treated areas, a sharp demarcation was seen with a sudden increase in the number of cones, more intense cone arrestin immunolabeling, and improved morphology of the cones when moving out of the transduced area (Fig 5D₁₋₂). Outside the injected region, cone density and morphology was normal (Fig 5E₁₋₂). Despite extended areas of cone loss, there were within the injection margin of the GFP labeled retina, some patches of surviving, but structurally compromised cones that expressed GFP (Fig 5F₁₋₃, arrows).

rAAV2/5-CBA-GFP—Cone arrestin immunolabeling showed a prominent decrease in cone density and altered cellular morphology at the border of the transduced region in retina of E1050-L treated with 4.70×10^{12} vg/ml of viral construct (Fig 6B₁₋₃). Within the central region of the transduced area, rare cones were found, and ONL thickness was reduced (Fig 6B₄). Confocal microscopy imaging of this same retina (Fig 6C₁₋₃) showed that some of the remaining cones expressed GFP (Fig 6C₃, arrows), and that both rods and cones had abnormally short IS, and had lost their OS. A ten-fold reduction in the titer of the viral vector delivered (4.70×10^{11} vg/ml), achieved potent and widespread transduction that was limited to rods and RPE, and did not alter PR morphology (Fig 6C₄).

DISCUSSION

This study compared the effectiveness and cell-specificity of three promoters (mOP, hGRK1, and CBA) in driving the expression of GFP in rods when packaged in a rAAV2/5 vector, and delivered via subretinal injection to the canine eye. Both mOP and hGRK1 enabled rod-specific expression of the transgene. Some degree of inflammation was observed with all constructs, and cone toxicity was found with the highest titers when hGRK1 and CBA promoters were used. Efficient transduction and limited ocular side-effects were achieved with lower titers.

Although chimeric rAAV have been developed to enhance cell-specific tropism, there is currently no single AAV serotype for which the capsid proteins enable restricted transduction of PR cells. rAAV2/5 is no exception, with tropism primarily directed towards RPE and PRs. In this study we also report that rAAV2/5 carrying the CBA promoter can drive low GFP expression in other retinal cells (Müller, ganglion, and horizontal cells). Thus, there is a need for cell-specific promoters that can further increase the safety of the viral constructs by turning on transgene expression solely in the targeted cells.

In most injected eyes, clinical signs of ocular inflammation were observed approximately 6 weeks post-injection. These ranged from increase in retinal vessel diameter, to focal damage in the bleb region with occasional retinal detachment, and these more severe lesions were confirmed by histology. Ocular inflammation was closely associated with dose, and was more frequent with the higher vector titers. Although this same vector serotype has been previously used at titers as high as 1.36×10^{13} vg/ml without causing any side-effects in normal adult canine retinas,²¹ we cannot exclude that the late-onset complications observed in this study may have been triggered by an immune reaction towards rAAV2/5 capsid proteins.²⁴ Another possibility is that high expression of the transgene GFP may be immunogenic. This has been suggested by Bainbridge and associates¹² who observed

similar late-onset complications in the canine retina following subretinal delivery of an rAAV2/2-CMV-GFP construct. The absence of such inflammatory responses in the study that used rAAV2/5 vectors to target GFP expression in cones may be explained by the lower levels of overall transgene expression in comparison to that achieved when only rods are transduced.²¹ Further investigation of the occurrence of potential immune reactions to either capsid proteins or the transgene following subretinal injections of rAAV2/5 vectors is warranted.

When delivered by means of an rAAV2/2 vector, the proximal region of the mouse opsin promoter has been shown to target transgene expression to rods and cones in rodents after subretinal delivery.²⁵ More recently, studies have demonstrated GFP reporter gene expression in rods and cones of both mice and rats when packaged into a rAAV2/5 vector.^{18, 26} Here, we provide the first report on the use of this promoter in a large animal model, and show that in the dog, contrary to what is observed in rodents, mOP restricts gene expression predominantly to rods. This finding highlights differences in cell-tropism across species, and supports the need for testing every new viral construct (i.e., new viral pseudotype, or new promoter) in a variety of animal models, including non-human primates, prior to the initiation of clinical trials in man. The rationale for using the dog to evaluate new viral vectors lies in the possibility for subsequently testing viral vector-mediated gene therapy for various naturally-occurring forms of retinal degeneration in this animal model. At the highest titer used in this study (3.27×10^{13} vg/ml), low levels of GFP expression were detected by immunohistochemistry in cells of the INL, IPL, and GCL. Transgene expression, and detection of rAAV genome and intact viral particles outside of the area of the subretinal injection has led some to suggest that rAAV vectors may potentially disseminate beyond the targeted cell population via transsynaptic transport.^{13, 27, 28}

The G-protein-coupled receptor protein kinase 1 (GRK1) promoter targets transgene expression to both rods and cones in mice when incorporated in a rAAV2/5 vector.¹⁹ In the canine retina, we now show that this promoter drives expression of the reporter gene exclusively in rods, except when high viral vector titers are used. This discrepancy may be explained by the species-specific differences in expression of G-protein coupled receptor kinases in rods and cones. Indeed, while GRK1 is expressed in both populations of PRs in mice and rats, it is only found in rods of the canine and pig retina.²⁹ Desensitization of cones in these species occurs via GRK7, a cone-specific GRK. In monkey and human retinas on the other hand, GRK1 is localized to rods, and also is co-expressed with GRK7 in cones.²⁹ These inter-species differences need to be taken into account when extrapolating results obtained in animal models to human. The lack of GRK1 expression in canine cones precludes evaluating viral vector constructs carrying the hGRK1 promoter for gene therapy targeted at cones in this animal model. While such a limitation may not be a concern when using rodent models, the lack of redundant GRK isoforms in rats and mice, may be responsible for the high activity of the hGRK1 promoter in cones. The contribution of GRK1 to the overall cone GRK activity in primates is unknown. For that reason, it is important to evaluate both hGRK1 and the mOP promoters for targeting specificity in the non-human primate retina.

The constitutive CMV immediate early promoter/enhancer has been widely used in gene therapy studies. When introduced into a rAAV2/5 vector, this promoter enables gene expression primarily in the RPE and PRs in the murine and canine retina^{3, 16} Because the CMV promoter can be silenced via DNA methylation,³⁰ a hybrid promoter composed of the CMV enhancer coupled to the chicken beta actin proximal promoter was used in this study. We confirm that this ubiquitously active promoter enables transgene expression primarily in the RPE and PRs (both rods and cones), but also at lower levels in horizontal, Müller, and ganglion cells. Transduction of Müller and ganglion cells with rAAV2/5-CBA-GFP has

been reported following intravitreal injection in the mouse.³¹ Thus, we cannot exclude that the targeting of inner retinal cells may have been caused by some degree of reflux of the viral solution from the subretinal space into the vitreal cavity.

Cone toxicity was induced by high titers of viral constructs carrying either the hGRK1 or CBA promoters. This toxicity was limited to the retinal region where the subretinal bleb was formed, and resulted in a prominent loss of cones and decreased expression of cone arrestin in the remaining cells. Such a finding could be easily overlooked if solely assessing retinal toxicity on H&E stained sections, particularly in species that have low cone-to-rod ratios. Our finding highlights the need for proper evaluation of the density and morphology of the various retinal cell populations, when testing novel viral vectors in the context of preclinical studies and safety trials. There is evidence from studies conducted in mouse, rat, guinea pig, ferret and dog retinas that AAV2/5 vectors can mediate gene transfer to cones.^{19–21} In primates, the absence of expression in cones of the AAV5 receptor, platelet-derived growth factor receptor alpha (PDGFR-A), is thought to be the molecular basis for selective tropism of this serotype to rods.¹⁵ However, this explanation seems to be challenged by a recent study in which an rAAV2/5 vector containing the L opsin gene under the control of the L/M opsin promoter and enhancer was shown to efficiently transduce primate cones.³² This cone transduction barrier does not appear to exist in the canine retina either, as there is good evidence that the AAV2/5 pseudotype which expresses the same capsid proteins that are recognized by PDGFR-A, is an efficient vector for cone-targeted gene therapy.^{21, 23}

At present, we do not know the cause for the dose-related cone toxicity seen with the hGRK1 and CBA promoters. When elevated viral titers in the order of 10^{12} – 10^{13} vg/ml were administered, a severe decrease in the density of cones, particularly in the center of the injected area was observed with both promoters. Yet, rare cones expressing the GFP transgene were found surviving close to the border region of the bleb. This observation was particularly surprising with the hGRK1 promoter as no transgene expression was seen in cones with lower titers (see above). Although rod loss was also observed in those areas treated with high viral titers, the effect appeared to be more severe on cones. However, this might simply reflect the lower density of cones versus rods in the canine retina. Cone loss may occur, following rod death, through a bystander effect (loss of structural/trophic support). Yet, it is also possible that cones are more sensitive to elevated levels of GFP expression. One plausible mechanism for this toxicity is that highly efficient transduction of GFP driven by these two promoters could overwhelm the translational machinery of cones and leads to their death.

The findings emphasize the importance of selecting the optimal promoters with the goal of maximizing specific transduction, and minimizing adverse sequelae. Proposing a titer that achieves optimal transduction requires reconciling the need to attain sustained and potent transgene expression while, at the same time, delivering a dose of viral vector that is not retinotoxic. Although this study did not quantitatively evaluate the levels of GFP expression, nor the percentage of rods that were efficiently transduced in the bleb region, the results support using the rAAV2/5-mOP, rAAV2/5-hGRK1, and rAAV2/5-CBA constructs at a titer of 3.27×10^{11} vg/ml, 1.51×10^{11} vg/ml, and 4.79×10^{11} vg/ml, respectively. Cautious comparison of the two rod-specific promoters (mOP and hGRK1) would suggest that higher transgene expression levels are achieved with rAAV2/5-hGRK1.

In summary, this study demonstrates that two rod-specific promoters (mOP, and hGRK1) can be used in a rAAV2/5 vector to efficiently target this cell population in the canine retina. It also identifies optimal viral titers that can induce high level of transgene expression without causing any significant clinical or histopathological complications (summarized in Fig 7). These results, together with the recent development and validation of viral constructs

that enable gene transduction in cones,²¹ has widened the palette of rAAV2/5 vectors available to target the various populations of PRs in dogs. This is particularly relevant for on-going preclinical studies aimed at developing corrective gene therapy approaches for *RHO* autosomal dominant RP, and *RPGR* X-linked RP.

MATERIAL & METHODS

rAAVvector production and purification

Three different promoters driving humanized green fluorescent protein (GFP) were evaluated in recombinant adeno-associated virus vector of serotype 5 (rAAV2/5). These included a 476 nt fragment of the proximal mouse opsin promoter from positions 944–1420 (mOP, Genbank Accession no 55171), a 292 nt segment (positions 1793 to 2087) of the human G-protein-coupled receptor protein kinase 1 promoter (hGRK1, GenBank AY327580), and the cytomegalovirus (CMV) immediate early enhancer combined with the chicken beta actin proximal promoter (referred throughout the text as CBA promoter)³³. These fragments were ligated into a recombinant AAV vector plasmid containing a SD/SA, GFP and polyadenylation sites. The resulting plasmid DNA constructs (mOP-GFP-rAAV, hGRK1-GFP-rAAV, and CBA-GFP-rAAV) (Figure 1) were then packaged into rAAV particles using standard vector preparation methods,^{34, 35} and titered for DNase-resistant vector genomes by Real-Time PCR relative to a standard. For these three plasmids, a pair of oligonucleotides was synthesized that target the SV40 polyadenylation signal (Forward: 5'-TTTGTGAAATTTGTGATGCT-3'; Reverse: 5'-TGAATGCAATTGTTGTTGTT-3'; PCR product: 85 base pairs). Along with these primers a reaction mix was set up using iQ SYBR® Green Supermix (Bio-Rad Laboratories, Hercules, CA). The reaction was performed in a MyiQ™ Real-Time PCR Detection System (Bio-Rad Laboratories, Hercules, CA), and the data was collected and titer calculated using the MyiQ™ Optical System Software, (Bio-Rad Laboratories Hercules, CA). The standard used for the Real-Time PCR was an AAV with a known titer that was independently verified by PCR, dot blot and Infectious Center Assay (Univ. Florida Vector Core facility). Finally, the purity of the vector was validated using three standard assays. First by silver-stained SDS-PAGE to confirm presence of only the 3 capsid proteins; secondly, by assay screening for bioburden by spreading 10 µL of the final product on a non-selective LB-agar plate; and lastly, the final product was assayed for endotoxin using the Endosafe-PTS, portable test system (Charles River Laboratories, Charleston, SC, USA). Viral vector stocks were kept at -80 °C in Balance Salt Solution (BSS; Alcon, Fort Worth, TX), and all subsequent dilutions were done using BSS.

Animals

Both eyes of 8 non-affected crossbred dogs were used for this study (see Table I). The animals were bred and/or maintained at the Retinal Disease Studies Facility (RDSF, New Bolton Center, University of Pennsylvania, Kennett Square, PA), and all procedures were in compliance with the ARVO statement for the Use of Animals in Ophthalmic and Vision Research.

Subretinal injections and clinical examinations

Subretinal injections of rAAV2/5 carrying 3 different promoter constructs driving the GFP reported gene were performed under general anesthesia following previously published procedures.^{21, 36} A total of volume of 150 µl of the viral vector solution was delivered under direct visualization with an operating microscope via a transvitreal approach without vitrectomy using a Retinaject subretinal injector (SurModics Inc., Eden Prairie, MN). Visualization of the fundus was achieved with either a Machemer magnifying vitrectomy lens (OMVI; Ocular Instruments Inc., Bellevue, WA), or a vitreoretinal surgery contact lens

(Acrivet Vit.Lens; Acrivet, Salt Lake City, UT). Several concentrations of each of the rAAV preparations were injected to determine the lowest titers capable of achieving sufficient expression of GFP in the targeted PRs (see titers in Table 1). As previous reports from our group have shown that subretinal injection of 150 μ l of isotonic sodium chloride solution is safe and does not cause any structural alterations in the dog,^{36, 37} no virus-free vehicle controls were included in the current study. At the time of the injection it was noted whether a subretinal bleb was formed, and its location and extent were recorded on a diagram of the animal's fundus (Figure 2A). Failed subretinal injections caused by either a sub-RPE injection, or by reflux into the vitreous, were also recorded. An anterior chamber paracentesis was immediately performed after the injection to prevent any increase in intraocular pressure, and a subconjunctival injection of 4 mg of triamcinolone acetonide was done in each eye.

Ophthalmic examinations, including biomicroscopy, indirect ophthalmoscopy, and fundus photography (Figs 2B₁₋₂, C₁₋₂) were conducted on a regular basis throughout the injection-termination time interval. Postoperative topical medication included application of atropine sulfate 1% drops once daily for 6 days, and prednisolone acetate 1% drops twice daily for 18 days. Systemic antibiotics (amoxicillin trihydrate/clavulanate potassium 20 mg/kg) were given orally twice daily for 1 week, and prednisolone oral solution (0.5 mg/kg) was administered twice daily for 5 days, followed by once daily for 1 week. Animals that showed signs of ocular inflammation after the completion of this initial treatment received a second subconjunctival injection of triamcinolone, oral administration of prednisolone, with or without topical application of prednisolone acetate 1%, and atropine sulfate 1%. In one case where improvement did not occur in one eye after the second round of treatment (Table 1; dog E1050), euthanasia was performed and eyes collected.

Tissue processing, histology, and immunohistochemistry

Dogs were euthanatized by intravenous injection of pentobarbital sodium. After enucleation, the globes were fixed and processed as previously described.³⁸ Briefly, a slit was made through the globe at the level of the ora serrata and the entire eye was immersed in 4% paraformaldehyde in 0.1 M phosphate-buffered saline (PBS) for 1 hour, the posterior eyecup was then separated and fixed for two additional hours, followed by overnight fixation in 2% paraformaldehyde. The eyecup was trimmed using the peri-operative diagrams that illustrated the placement and extent of the subretinal bleb as a guide (Figure 2A), and tissues cryoprotected in gradient concentrations of sucrose diluted in 0.1 M PBS, prior to embedding in optimal cutting temperature (OCT) medium. Cryosections (10- μ m thick) that included both the area of the previous subretinal bleb and non-injected regions, were cut and stained with H&E for histological assessment, or used for evaluation of GFP expression, and immunohistochemistry (IHC) as described below.

Native GFP expression was assessed by examining unstained sections with an epifluorescence microscope (Axioplan; Carl Zeiss Meditech, Oberkochen, Germany). To identify whether low levels of GFP expression were present in the retina but not detected on unlabeled sections, IHC directed against GFP was carried out using a polyclonal rabbit antibody (1:1 000; provided by W Clay Smith). Co-labeling with a rabbit polyclonal antibody directed against human cone arrestin (LUMIf; 1/10 000 provided by Cheryl Craft) was also performed to identify cones transduced by the viral vectors. The antigen-antibody complexes were visualized with fluorochrome-labeled secondary antibodies (Alexa Fluor, 1:200; Molecular Probes, Eugene, OR, USA), and DAPI stain was used to detect cell nuclei. Slides were mounted with gelvatol, a medium composed of polyvinyl alcohol and DABCO (Sigma-Aldrich, St Louis, MO, USA), coverslipped, and examined by epifluorescence microscopy. Images were digitally captured (Spot 4.0 camera, Diagnostic Instruments, Sterling Heights, MI), and imported into a graphics program (Photoshop; Adobe, Mountain

View, CA, USA) for display. When precise localization of transgene expression was needed, sections were also imaged by confocal microscopy using a Leica TCS-SP5 tunable confocal system with a Leica DM 6000 CFS upright microscope (Leica Microsystems, Wetzlar, Germany) through a 40x oil lens and a 1.25 numerical aperture. The specimens were excited at 488 nm and 543 nm, respectively, with Argon and Helium Neon lasers.

Acknowledgments

The authors are grateful to Dr. Lingli Zhang (Veterinary Imaging Core Facility, University of Pennsylvania) for assistance with confocal microscopy, Dr. Cheryl Craft (University of Southern California, Los Angeles) for providing the human cone arrestin antibody, Dr W Clay Smith (University of Florida) for the polyclonal GFP antibody, Svetlana Savina for histotechnical assistance, the staff of the RDSF facility for help with animal resources, Lydia Melnyk for research coordination, and Mary Leonard (Biomedical Art and Design facility, University of Pennsylvania) for the illustrations. This work was supported by: NIH grants EY06855, EY13132, EY17549, RR02512, P30EY-001583, The Foundation Fighting Blindness Individual Investigator and Center grants (TA-NP-0607-0393-UPA; C-CMM-04090476-UPA02, and TA-GT-0507-0384-UFL), The Fight for Sight Nowak family grant, Hope for Vision Foundation, and the ONCE International Prize for R&D in Biomedicine and New Technologies for the Blind.

References

1. Acland GM, Aguirre GD, Ray J, Zhang Q, Aleman TS, Cideciyan AV, et al. Gene therapy restores vision in a canine model of childhood blindness. *Nat Genet.* 2001; 28(1):92–95. [PubMed: 11326284]
2. Pang JJ, Chang B, Kumar A, Nusinowitz S, Noorwez SM, Li J, et al. Gene therapy restores vision-dependent behavior as well as retinal structure and function in a mouse model of RPE65 Leber congenital amaurosis. *Mol Ther.* 2006; 13(3):565–572. [PubMed: 16223604]
3. Weber M, Rabinowitz J, Provost N, Conrath H, Folliot S, Briot D, et al. Recombinant adeno-associated virus serotype 4 mediates unique and exclusive long-term transduction of retinal pigmented epithelium in rat, dog, and nonhuman primate after subretinal delivery. *Mol Ther.* 2003; 7(6):774–781. [PubMed: 12788651]
4. Bainbridge JW, Smith AJ, Barker SS, Robbie S, Henderson R, Balaggan K, et al. Effect of gene therapy on visual function in Leber's congenital amaurosis. *N Engl J Med.* 2008; 358(21):2231–2239. [PubMed: 18441371]
5. Maguire AM, Simonelli F, Pierce EA, Pugh EN Jr, Mingozzi F, Bennicelli J, et al. Safety and efficacy of gene transfer for Leber's congenital amaurosis. *N Engl J Med.* 2008; 358(21):2240–2248. [PubMed: 18441370]
6. Hauswirth W, Aleman TS, Kaushal S, Cideciyan AV, Schwartz SB, Wang L, et al. Treatment of leber congenital amaurosis due to RPE65 mutations by ocular subretinal injection of adeno-associated virus gene vector: short-term results of a phase I trial. *Hum Gene Ther.* 2008; 19(10):979–990. [PubMed: 18774912]
7. Surace EM, Auricchio A. Versatility of AAV vectors for retinal gene transfer. *Vision Res.* 2008; 48(3):353–359. [PubMed: 17923143]
8. Hildinger M, Auricchio A, Gao G, Wang L, Chirmule N, Wilson JM. Hybrid vectors based on adeno-associated virus serotypes 2 and 5 for muscle-directed gene transfer. *J Virol.* 2001; 75(13):6199–6203. [PubMed: 11390622]
9. Beltran WA. The use of canine models of inherited retinal degeneration to test novel therapeutic approaches. *Vet Ophthalmol.* 2009; 12(3):192–204. [PubMed: 19392879]
10. Narfstrom K, Katz ML, Bragadottir R, Seeliger M, Boulanger A, Redmond TM, et al. Functional and structural recovery of the retina after gene therapy in the RPE65 null mutation dog. *Invest Ophthalmol Vis Sci.* 2003; 44(4):1663–1672. [PubMed: 12657607]
11. Acland GM, Aguirre GD, Bennett J, Aleman TS, Cideciyan AV, Bennicelli J, et al. Long-term restoration of rod and cone vision by single dose rAAV-mediated gene transfer to the retina in a canine model of childhood blindness. *Mol Ther.* 2005; 12(6):1072–1082. [PubMed: 16226919]

12. Bainbridge JW, Mistry A, Schlichtenbrede FC, Smith A, Broderick C, De Alwis M, et al. Stable rAAV-mediated transduction of rod and cone photoreceptors in the canine retina. *Gene Ther.* 2003; 10(16):1336–1344. [PubMed: 12883530]
13. Stieger K, Colle MA, Dubreil L, Mendes-Madeira A, Weber M, Le Meur G, et al. Subretinal Delivery of Recombinant AAV Serotype 8 Vector in Dogs Results in Gene Transfer to Neurons in the Brain. *Mol Ther.* 2008; 16(5):916–923. [PubMed: 18388922]
14. Natkunarajah M, Trittibach P, McIntosh J, Duran Y, Barker SE, Smith AJ, et al. Assessment of ocular transduction using single-stranded and self-complementary recombinant adeno-associated virus serotype 2/8. *Gene Ther.* 2008; 15(6):463–467. [PubMed: 18004402]
15. Lotery AJ, Yang GS, Mullins RF, Russell SR, Schmidt M, Stone EM, et al. Adeno-associated virus type 5: transduction efficiency and cell-type specificity in the primate retina. *Hum Gene Ther.* 2003; 14(17):1663–1671. [PubMed: 14633408]
16. Yang GS, Schmidt M, Yan Z, Lindbloom JD, Harding TC, Donahue BA, et al. Virus-mediated transduction of murine retina with adeno-associated virus: effects of viral capsid and genome size. *J Virol.* 2002; 76(15):7651–7660. [PubMed: 12097579]
17. Li W, Kong F, Li X, Dai X, Liu X, Zheng Q, et al. Gene therapy following subretinal AAV5 vector delivery is not affected by a previous intravitreal AAV5 vector administration in the partner eye. *Mol Vis.* 2009; 15:267–275. [PubMed: 19190735]
18. Glushakova LG, Timmers AM, Issa TM, Cortez NG, Pang J, Teusner JT, et al. Does recombinant adeno-associated virus-vectored proximal region of mouse rhodopsin promoter support only rod-type specific expression in vivo? *Mol Vis.* 2006; 12:298–309. [PubMed: 16617297]
19. Khani SC, Pawlyk BS, Bulgakov OV, Kasperek E, Young JE, Adamian M, et al. AAV-mediated expression targeting of rod and cone photoreceptors with a human rhodopsin kinase promoter. *Invest Ophthalmol Vis Sci.* 2007; 48(9):3954–3961. [PubMed: 17724172]
20. Li Q, Timmers AM, Guy J, Pang J, Hauswirth WW. Cone-specific expression using a human red opsin promoter in recombinant AAV. *Vision Res.* 2008; 48(3):332–338. [PubMed: 17905404]
21. Komaromy AM, Alexander JJ, Cooper AE, Chiodo VA, Acland GM, Hauswirth WW, et al. Targeting gene expression to cones with human cone opsin promoters in recombinant AAV. *Gene Ther.* 2008
22. Petersen-Jones SM, Bartoe JT, Fischer AJ, Scott M, Boye SL, Chiodo V, et al. AAV retinal transduction in a large animal model species: comparison of a self-complementary AAV2/5 with a single-stranded AAV2/5 vector. *Mol Vis.* 2009; 15:1835–1842. [PubMed: 19756181]
23. Komaromy, AM.; Alexander, JJ.; Chiodo, VA.; Garcia, MM.; Tanaka, JC.; Craft, CM., et al. ARVO. Fort Lauderdale, FL: April 28. 2008 Long-term rescue of cone function in a canine model of achromatopsia by rAAV-mediated gene therapy; p. 2008E-abstract # 1131
24. Vandenberghe LH, Wilson JM. AAV as an immunogen. *Curr Gene Ther.* 2007; 7(5):325–333. [PubMed: 17979679]
25. Flannery JG, Zolotukhin S, Vaquero MI, LaVail MM, Muzyczka N, Hauswirth WW. Efficient photoreceptor-targeted gene expression in vivo by recombinant adeno-associated virus. *Proc Natl Acad Sci U S A.* 1997; 94(13):6916–6921. [PubMed: 9192666]
26. Allocca M, Mussolino C, Garcia-Hoyos M, Sanges D, Iodice C, Petrillo M, et al. Novel adeno-associated virus serotypes efficiently transduce murine photoreceptors. *J Virol.* 2007; 81(20):11372–11380. [PubMed: 17699581]
27. Provost N, Le Meur G, Weber M, Mendes-Madeira A, Podevin G, Cherel Y, et al. Biodistribution of rAAV vectors following intraocular administration: evidence for the presence and persistence of vector DNA in the optic nerve and in the brain. *Mol Ther.* 2005; 11(2):275–283. [PubMed: 15668139]
28. Stieger K, Schroeder J, Provost N, Mendes-Madeira A, Belbellaa B, Le Meur G, et al. Detection of intact rAAV particles up to 6 years after successful gene transfer in the retina of dogs and primates. *Mol Ther.* 2009; 17(3):516–523. [PubMed: 19107120]
29. Weiss ER, Ducceschi MH, Horner TJ, Li A, Craft CM, Osawa S. Species-specific differences in expression of G-protein-coupled receptor kinase (GRK) 7 and GRK1 in mammalian cone photoreceptor cells: implications for cone cell phototransduction. *J Neurosci.* 2001; 21(23):9175–9184. [PubMed: 11717351]

30. Brooks AR, Harkins RN, Wang P, Qian HS, Liu P, Rubanyi GM. Transcriptional silencing is associated with extensive methylation of the CMV promoter following adenoviral gene delivery to muscle. *J Gene Med.* 2004; 6(4):395–404. [PubMed: 15079814]
31. Pang JJ, Lauramore A, Deng WT, Li Q, Doyle TJ, Chiodo V, et al. Comparative analysis of in vivo and in vitro AAV vector transduction in the neonatal mouse retina: effects of serotype and site of administration. *Vision Res.* 2008; 48(3):377–385. [PubMed: 17950399]
32. Mancuso K, Hauswirth WW, Li Q, Connor TB, Kuchenbecker JA, Mauck MC, et al. Gene therapy for red-green colour blindness in adult primates. *Nature.* 2009; 461(7265):784–787. [PubMed: 19759534]
33. Kiwaki K, Kanegae Y, Saito I, Komaki S, Nakamura K, Miyazaki JI, et al. Correction of ornithine transcarbamylase deficiency in adult spf(ash) mice and in OTC-deficient human hepatocytes with recombinant adenoviruses bearing the CAG promoter. *Hum Gene Ther.* 1996; 7(7):821–830. [PubMed: 8860834]
34. Zolotukhin S, Potter M, Hauswirth WW, Guy J, Muzyczka N. A “humanized” green fluorescent protein cDNA adapted for high-level expression in mammalian cells. *J Virol.* 1996; 70(7):4646–4654. [PubMed: 8676491]
35. Zolotukhin S, Byrne BJ, Mason E, Zolotukhin I, Potter M, Chesnut K, et al. Recombinant adeno-associated virus purification using novel methods improves infectious titer and yield. *Gene Ther.* 1999; 6(6):973–985. [PubMed: 10455399]
36. Komaromy AM, Varner SE, de Juan E, Acland GM, Aguirre GD. Application of the new subretinal injection device in the dog. *Cell Transplantation.* 2006; 15:511–519. [PubMed: 17121162]
37. Komaromy AM, Acland GM, Aguirre GD. Operating in the dark: a night-vision system for surgery in retinas susceptible to light damage. *Arch Ophthalmol.* 2008; 126(5):714–717. [PubMed: 18474785]
38. Beltran WA, Hammond P, Acland GM, Aguirre GD. A frameshift mutation in *RPGR* exon ORF15 causes photoreceptor degeneration and inner retina remodeling in a model of X-linked retinitis pigmentosa. *Invest Ophthalmol Vis Sci.* 2006; 47(4):1669–1681. [PubMed: 16565408]

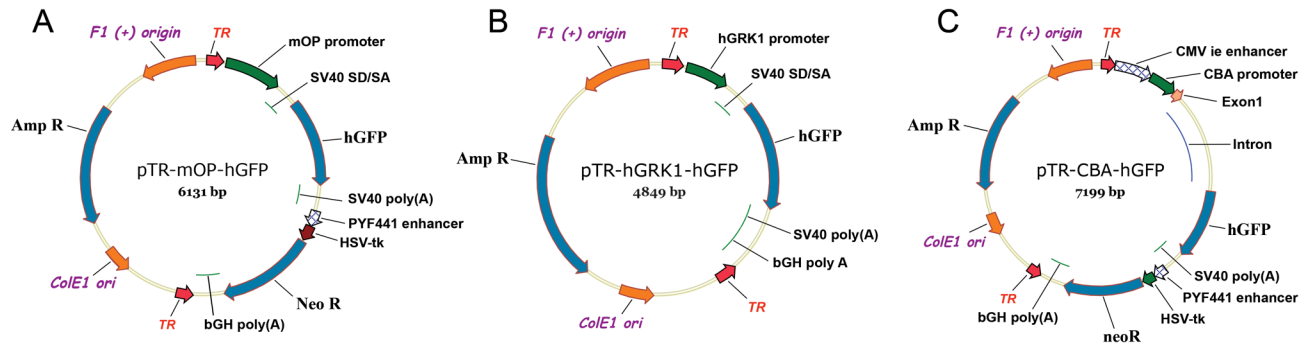


Figure 1. Schematic diagrams of the plasmid constructs used to produce rAAV

(A) Map of the pTR-mOP-hGFP plasmid DNA used to make the rAAV2/5-mOP-GFP virus.

(B) Map of the pTR-hGRK1-hGFP plasmid DNA used to make the rAAV2/5-hGRK1-GFP virus.

(C) Map of the pTR-CBA-hGFP plasmid DNA used to make the rAAV2/5-CBA-GFP virus.

TR represents AAV2 inverted terminal repeats; mOP represents a fragment of the proximal mouse opsin promoter; hGRK1 represents a fragment of the human G-protein-coupled receptor protein kinase 1 promoter; CMV ie represents the cytomegalovirus immediate early enhancer; CBA represents the chicken beta-actin promoter; SV40 SD/SA represents the SV40 late viral protein gene 16S/19S splice donor and acceptor signal; hGFP represents the coding sequence of the humanized green fluorescence protein gene; SV40 (poly A) and bGH poly (A) represent polyadenylation signals; HSV-tk represents the thymidine kinase promoter of the herpes simplex virus, and Neo R represents the coding sequence of the neomycin resistance gene.

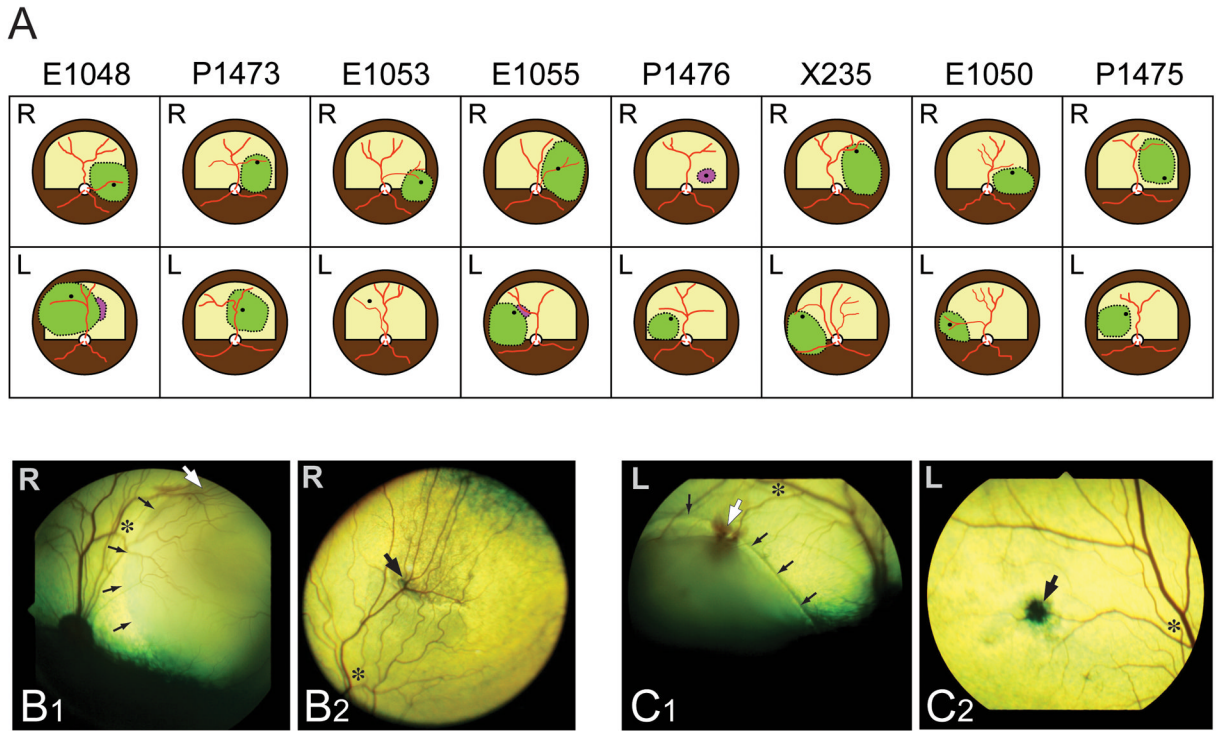


Figure 2. Location and extent of subretinal injections

(A) Diagrams of the fundus of the 16 eyes in which a subretinal injection was attempted. The green areas show the locations where subretinal blebs were achieved. The dark spot within the area of the subretinal bleb shows the location of the retinotomy. Purple areas show the location where some viral solution was seen injected under the RPE. [Note: the canine fundus is comprised of a tapetal region (superior; labeled in yellow; RPE non pigmented) and a non-tapetal region (inferior; labeled in brown; RPE pigmented)].

(B₁₋₂) Fundus photographs of the right eye of dog X235 immediately after performing the subretinal injection (B₁) and at termination (day 56; B₂). (C₁₋₂) Fundus photographs of the left eye of dog X235 immediately after performing the subretinal injection (C₁) and at termination (day 56; C₂). Asterisks show the same retinal location at time of injection and termination; small black arrows point to the edge of the subretinal bleb; large white arrows show the retinotomy site (at time of injection), and large black arrows point to the subsequent scar visible at termination.

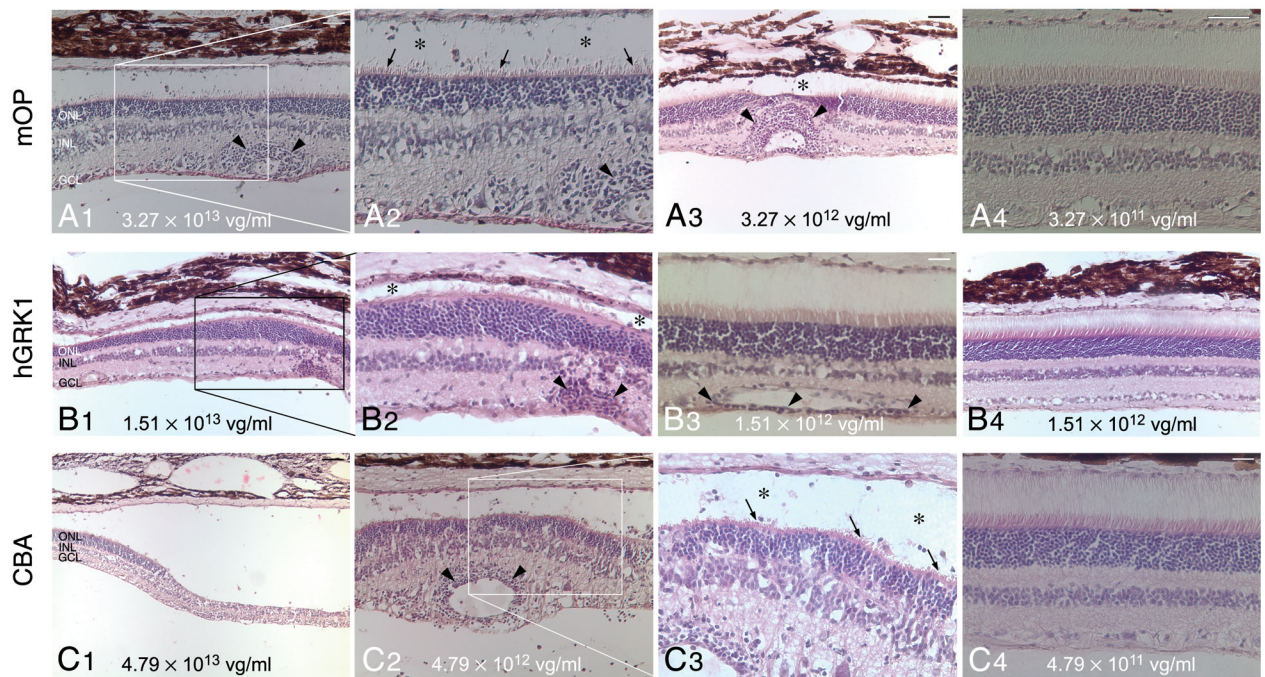


Figure 3. Histopathological findings following subretinal injection with three different rAAV2/5 constructs

(A₁₋₄) H&E stained retinal section of eyes treated with different titers of rAAV2/5-mOP-GFP: E1048-R (3.27×10^{13} vg/ml) (A₁₋₂); E1048-L (3.27×10^{12} vg/ml) (A₃); and P1473-R (3.27×10^{11} vg/ml) (A₄).

(B₁₋₄) H&E stained retinal section of eyes treated with different titers of rAAV2/5-hGRK1-GFP: E1055-R (1.51×10^{13} vg/ml) (B₁₋₂); P1476-L (1.51×10^{12} vg/ml) (B₃); and E1055-L (1.51×10^{12} vg/ml) (B₄).

(C₁₋₄) H&E stained retinal section of eyes treated with different titers of rAAV2/5-CBA-GFP: E1050-R (4.79×10^{13} vg/ml) (C₁); E1050-L (4.79×10^{12} vg/ml) (C₂₋₃); P1475-R (4.79×10^{11} vg/ml) (C₄).

Abbreviations: ONL, outer nuclear layer; INL, inner nuclear layer; GCL, ganglion cell layer. Scale bars: (A₁, A₃, A₄, B₁, B₄, C₂) 40 μ m; (B₃, C₄) 20 μ m; (C₁) 80 μ m.

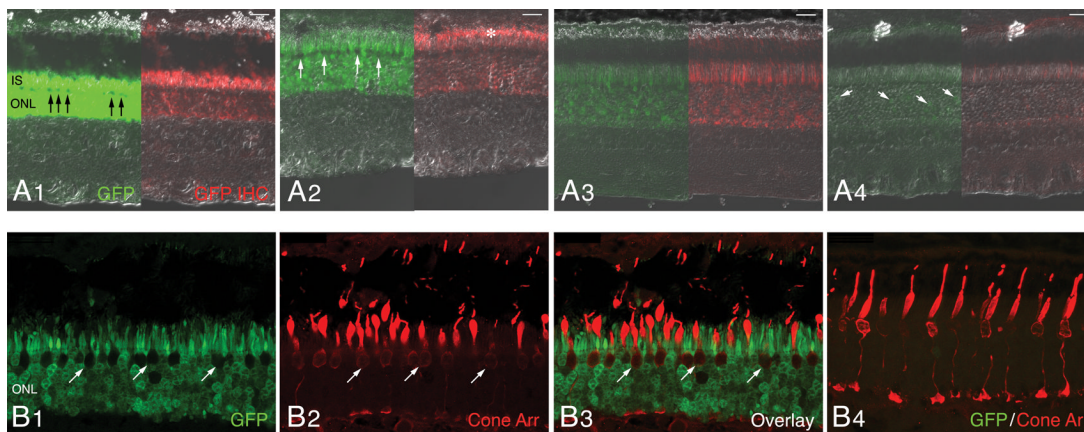


Figure 4. Transduction pattern of AAV2/5-mOP-GFP following subretinal delivery to the normal canine retina

Native GFP fluorescence (green) and GFP immunolabeling (red) images merged with DIC/ Nomarski optics; images show the GFP expression with decreasing viral vector titers (**A₁₋₄**). **A₁**) Retina of E1048-R (3.27×10^{13} vg/ml). **A₂**) Retina of E1048-L (3.27×10^{12} vg/ml). **A₃**) Retina of P1473-R (3.27×10^{11} vg/ml). **A₄**) Retina of P1473-L (3.27×10^{10} vg/ml).

Confocal microscopy images of native GFP (green) and cone arrestin (red) immunolabeling in the injected area (**B₁₋₃**) and non-injected area (**B₄**) of retina E1048-R.

Abbreviations: IS, inner segments; ONL, outer nuclear layer; GFP, green fluorescent protein; IHC, immunohistochemistry; Cone Arr. cone arrestin.

Scale bars: (**A₁₋₄**) 20 μ m; (**B₁₋₄**) 25 μ m.

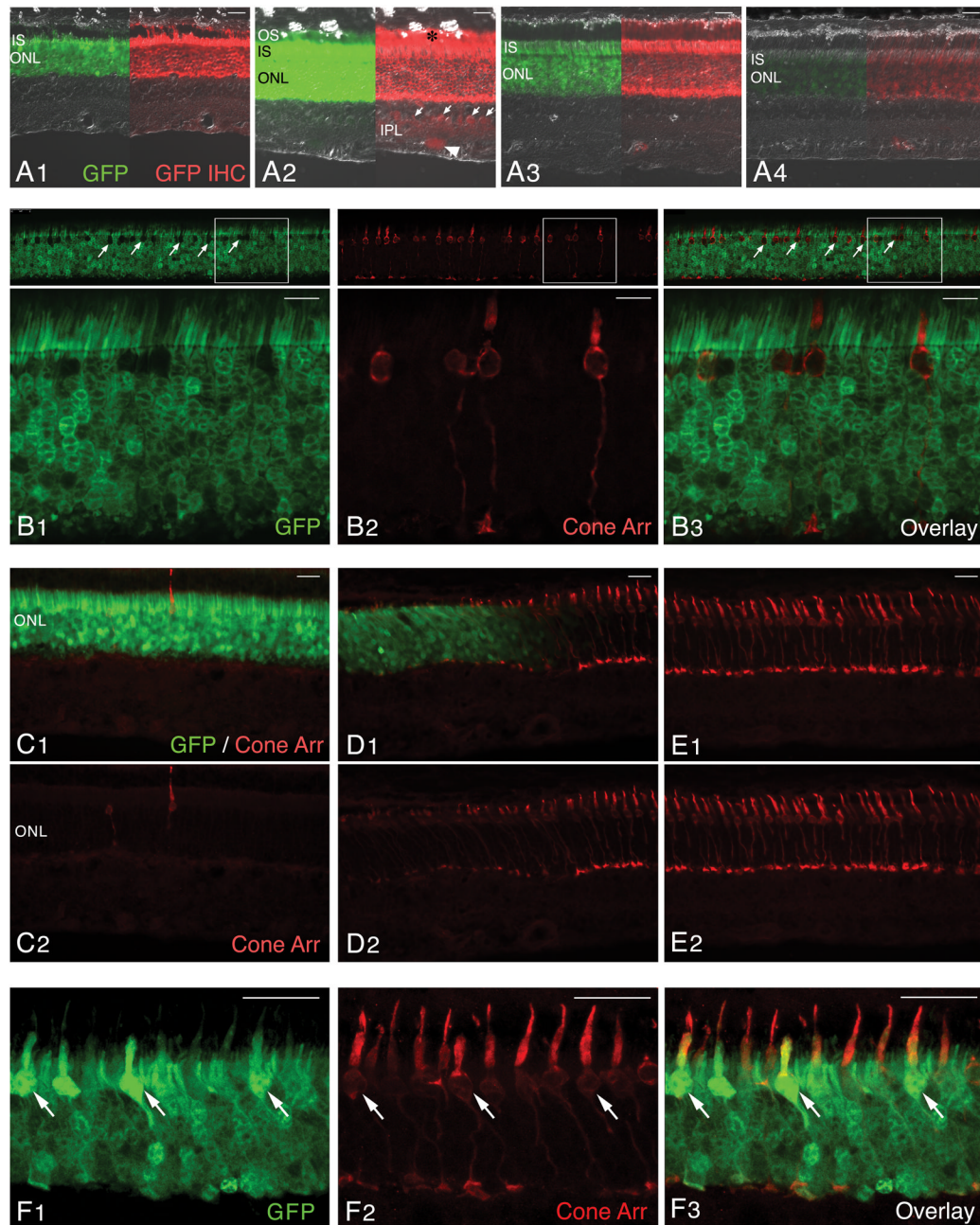


Figure 5. Transduction pattern of AAV2/5-hGRK1-GFP following subretinal delivery to the normal canine retina

(A₁₋₄) Native GFP fluorescence (green) and GFP immunolabeling (red) images merged with DIC/Nomarski optics; images show the GFP expression with decreasing viral vector titers.

(A₁) Retina of E1055-R (1.51×10^{13} vg/ml). (A₂) Retina of P1476-L (1.51×10^{12} vg/ml).

(A₃) Retina of X235-R (1.51×10^{11} vg/ml). (A₄) Retina of X235-L (1.51×10^{10} vg/ml).

(B₁₋₃) Confocal microscopy images of native GFP (green) and cone arrestin (red) immunolabeling in the injected area of retina P1476-L. (C–E) Epifluorescence microscopy images of native GFP (green) and cone arrestin (red) immunolabeling in the center (C₁₋₂), at the border (D₁₋₂), and outside the injected retinal area of E1055-R. (F₁₋₃) Confocal

microscopy images of native GFP (green) and cone arrestin (red) immunolabeling in the injected area of retina E1055-R.

Abbreviations: OS, outer segments; IS, inner segments; ONL, outer nuclear layer; INL; GFP, green fluorescent protein; IHC, immunohistochemistry; Cone Arr. cone arrestin.

Scale bars: (A₁₋₄; C₁₋₂, D₁₋₂, E₁₋₂) 20 μ m; (B₁₋₃) 10 μ m; (F₁₋₃) 25 μ m.

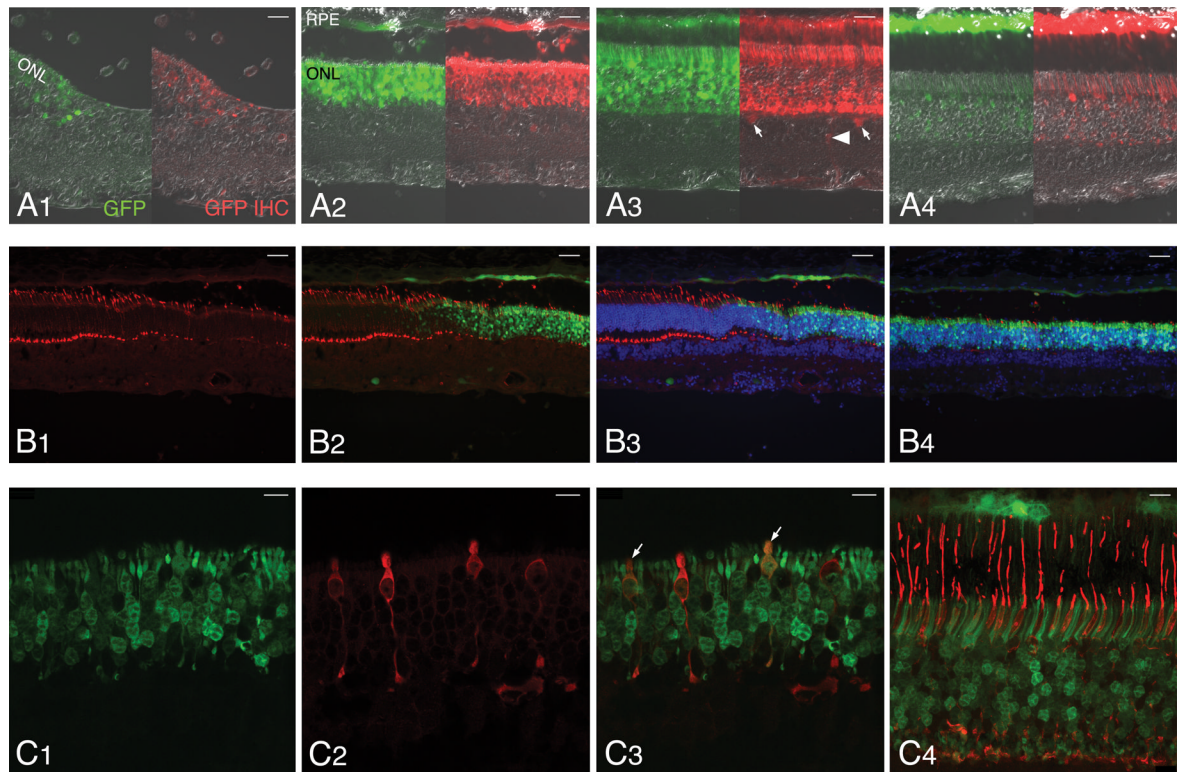


Figure 6. Transduction pattern of AAV2/5-CBA-GFP following subretinal delivery to the normal canine retina

Native GFP fluorescence (green) and GFP immunolabeling (red) images merged with DIC/ Nomarski optics; images show the GFP expression with decreasing viral vector titers (**A**₁₋₄). **A**₁) Retina of E1050-R (4.79×10^{13} vg/ml). **A**₂) Retina of E1050-L (4.79×10^{12} vg/ml). **A**₃) Retina of P1475-R (4.79×10^{11} vg/ml). **A**₄) Retina of P1475-L (4.79×10^{10} vg/ml).

Epifluorescence microscopy images at the border (**B**₁₋₃) and in the center (**B**₄) of the injected retinal area of E1050-L (4.79×10^{12} vg/ml). Confocal microscopy images of native GFP (green) and cone arrestin (red) immunolabeling in the injected area of retina E1050-L (4.79×10^{12} vg/ml) (**C**₁₋₃), and retina P1475-R (4.79×10^{11} vg/ml) (**C**₄).

Abbreviations: RPE, retinal pigment epithelium, ONL, outer nuclear layer; GFP, green fluorescent protein; IHC, immunohistochemistry; Cone Arr. cone arrestin.

Scale bars: (**A**₁₋₄) 20 μ m; (**B**₁₋₄) 40 μ m; (**C**₁₋₄) 10 μ m.

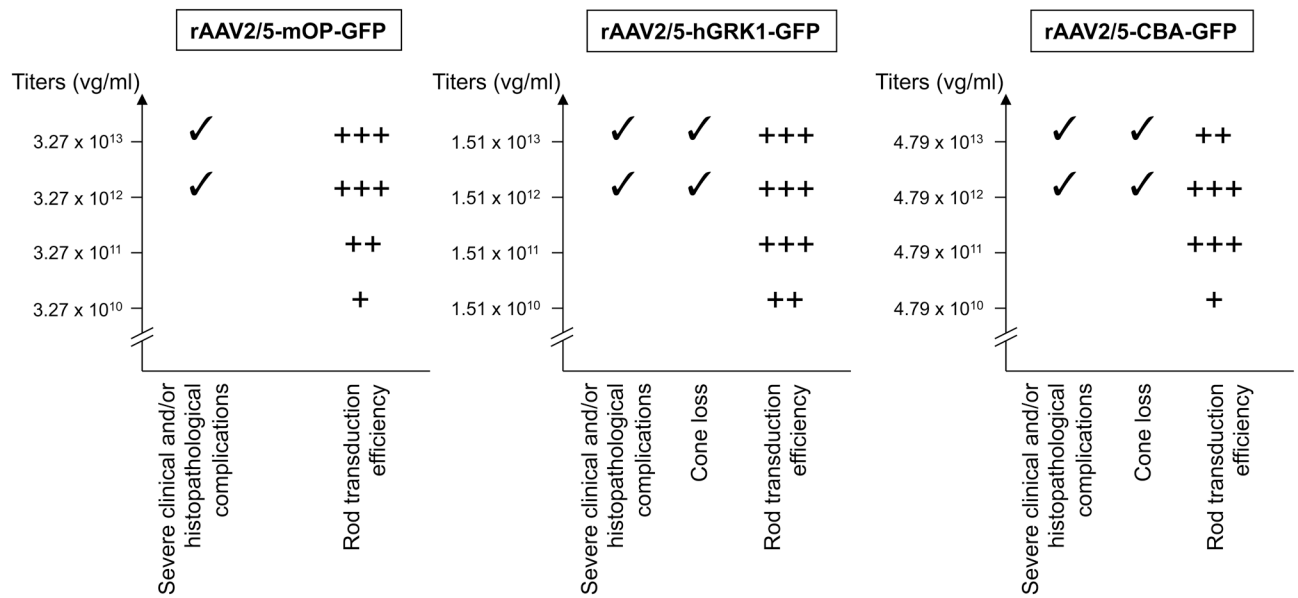


Figure 7. Summary of rod transduction efficiency and complications observed with the three viral vector constructs evaluated in this study. (A) rAAV2/5-mOP-GFP; (B) rAAV2/5-hGRK1-GFP; (C) rAAV2/5-CBA-GFP. +: limited; ++: moderate; +++: intense.

Table 1

Summary of dogs injected, promoters used, clinical findings, and sites of GFP expression.

Promoter	Dog	Sex	Eye	Age at injection (weeks)	Volume injected (µl)	Vector genomes per ml	Injection-termination interval (days)	Clinical findings (days to onset)	GFP expression in rods	Other sites of GFP expression
mOP500	E1048	M	R	11.4	150	3.27×10^{13}	55	None	Intense	INL cells, IPL
	E1048	M	L	11.4	150 ^a	3.27×10^{12}	55	Focal chorio-retinitis (7)	Intense	-
hGRK1	P1473	M	R	19.9	150	3.27×10^{11}	69	Dilated retinal vessels (43)	Moderate	-
	P1473	M	L	19.9	150	3.27×10^{10}	69	Dilated retinal vessels (43)	Limited	-
	E1053	M	R	12	150	1.51×10^{13}	48	Focal chorio-retinitis (41)	Intense	cones (few)
	E1053	M	L	12	150 ^b	1.51×10^{12}	48	Focal chorio-retinitis (41)	Intense*	-
CBA	E1055	F	R	12	150	1.51×10^{13}	48	Focal Retinitis + RD (41)	Intense	cones (few)
	E1055	F	L	12	150 ^d	1.51×10^{12}	48	Focal retinal vasculitis (41)	Intense	-
	P1476	F	R	19.9	150 ^c	1.51×10^{13}	69	Dilated retinal vessels (43)	Intense	-
	P1476	F	L	19.9	150	1.51×10^{12}	69	Dilated retinal vessels (43)	Intense	INL cells, IPL, GCs
	X235	F	R	16.6	150	1.51×10^{11}	56	None	Intense	-
CBA	X235	F	L	16.6	150	1.51×10^{10}	56	None	Moderate	-
	E1050	M	R	11.4	150	4.79×10^{13}	26	Focal retinal vasculitis (20) Panuveitis (23) + RD (26)	Moderate ^o	RPE, cones
	E1050	M	L	11.4	150	4.79×10^{12}	26	Focal tapetal discoloration (7)	Intense	RPE, cones, IPL, GCs, NFL
CBA	P1475	M	R	19.9	150	4.79×10^{11}	69	Dilated retinal vessels (43)	Intense	RPE, some cones horizontal cells, Müller cells, GCs, astrocytes, NFL
	P1475	M	L	19.9	150	4.79×10^{10}	69	Dilated retinal vessels (43)	Limited	RPE

Abbreviations: M, male; F, female; R, right; L, left; GFP, green fluorescent protein; RD, retinal detachment; IPL, inner plexiform layer; GCs, ganglion cells; RPE, retinal pigment epithelium, NFL, nerve fiber layer.

mOP500: mouse opsin promoter

hGRK1: human G-protein-coupled receptor protein kinase 1 promoter

CBA: CMV immediate early enhancer + chicken β actin proximal promoter

^a subretinal bleb well formed but with also some sub-RPE injection.

- b* no subretinal bleb formed, injected solution refluxed into the vitreous.
- c* no subretinal bleb formed, injected solution went sub-RPE → reflux into vitreous
- * , limited to rods at retinotomy site;
- ^o limited to rods at the border of retinal detachment.